



# Phase formation and properties of the LTCC composite based on the eutectic system BaO–ZnO–SiO<sub>2</sub>–B<sub>2</sub>O<sub>3</sub>

Song Chen\*, Shuren Zhang, Xiaohua Zhou, Ting Zhang, Ming He

School of Microelectronics and Solid State Electronics, University of Electronic Science and Technology of China, Chengdu 610054, People's Republic of China

## ARTICLE INFO

### Article history:

Received 3 January 2010  
Received in revised form 16 March 2010  
Accepted 17 March 2010  
Available online 23 March 2010

### Keywords:

Ceramics  
Sintering  
Thermal expansion  
Dielectric property  
X-ray diffraction  
SEM

## ABSTRACT

In this work, a low-temperature co-fired ceramic (LTCC) composite based on the eutectic system BaO–ZnO–SiO<sub>2</sub>–B<sub>2</sub>O<sub>3</sub> is fabricated. The phase formation in the LTCC composite is investigated by XRD, SEM and DSC technologies. Dielectric and thermal properties are discussed in terms of the phase composition. The results indicate that major mineral phases of the LTCC composite are barium silicate, willemite, SiO<sub>2</sub> crystal phases and additional quartz. Due to the peculiar physical characteristics of these mineral phases, the LTCC composite can express different dielectric and thermal properties along with the evolution of the major mineral phases.

© 2010 Elsevier B.V. All rights reserved.

## 1. Introduction

With further miniaturization of electronic devices, low-temperature co-fired ceramic (LTCC) materials, in recent years, are widely attracted to the application of semiconductor devices [1,2]. Specially, in order to achieve a thermal match between substrates and metallized wiring layers, a considerable CTE (not <10 ppm °C<sup>-1</sup>) [3] is expected to achieve. So far, glass–ceramics and ceramic/glass composites [4,5] have been widely researched for LTCC application due to their tailored physical properties and low sintering temperature. Nevertheless, the manufactures of glass materials are usually complex processes including melting, cooling and crystallization. The cost is also relatively high. Consequently, it should be considered by choosing more convenient methods to obtain LTCC materials. At present, a low-temperature sintering method [6,7] based on the eutectic system has the potential to improve the complex processes. The eutectic system with melting temperature not exceeding 1000 °C can supply a liquid-phase sintering aid for the fabrication of LTCC materials. On the basis of the liquid-phase sintering aid, the mineral phases with particular physical properties [8,9] can be available fabricated. Also, dielectric and thermal properties of LTCC materials can be designed in terms of their

phase composition. It is well known [10] that quartz is characterized by excellent dielectric characteristics (permittivity: 3.58) and high CTE (13.2 ppm °C<sup>-1</sup>, in the temperature range of 20 °C to 300 °C). Thus, quartz can be used to adjust the dielectric and thermal properties of LTCC materials as filler. In this work, we study the LTCC composite containing quartz based on the eutectic system BaO–ZnO–SiO<sub>2</sub>–B<sub>2</sub>O<sub>3</sub>. The main objective of the work is to investigate the correlation between the phase composition and the dielectric and thermal properties, and to develop a convenient method to fabricate LTCC materials.

## 2. Experimental

Reagent-grade raw materials of silicon acid, boric acid, zinc oxide, barium hydroxide octahydrate and quartz powder with purity higher than 99% were used as the starting materials. In this work, the de-ionized water was used.

According to the designed composition in Table 1, the above materials were weighed and milled with water for 7 h. The ratio of the water to solid was regulated to 3:2. Upon treatment, the slurries were dried and then were pre-sintered at 700 °C for 3 h. Subsequently, the pre-sintered powders with the particle size of 0.5–1.0 μm were molded into the specimens under a compressive stress of 25 MPa. Finally, the specimens were sintered continuously at 400 °C for 3 h, 700 °C for 3 h and selected densification temperature for 15 min. The as-sintered specimens were analyzed by using a scanning electron microscope (JSM-6490LV, Japan), an X-ray powder diffraction patterns and a differential scanning calorimetry (NETZSCH STA449C, Germany, heating at a rate of 10 °C min<sup>-1</sup>). The X-ray powder diffraction patterns were recorded on a D/Max-III A machine (Rigaku Industrial Corporation, Japan) using Cu Kα radiation (40 kV, 30 mA) with a scanning rate of 2° min<sup>-1</sup>. The CTE of the specimens were tested by a dilatometer (NETZSCH DIL402PC, Germany, heating at a rate of 3 °C min<sup>-1</sup>). Permittivity and dielectric loss were tested (1 MHz, at room-temperature) by a PRECISION LCR METER instrument (Agilent 4284A, U.S.A.).

\* Corresponding author at: School of Microelectronics and Solid State Electronics, University of Electronic Science and Technology of China, No. 4, Section 2, North Jianshe Road, Chengdu 610054, People's Republic of China. Tel.: +86 28 83208048. E-mail address: [chengdu20100@163.com](mailto:chengdu20100@163.com) (S. Chen).

**Table 1**  
The composition of the matrixes and the composites.

Specimen	Matrix composition (wt.%)	Addition of quartz (wt.%)
Z1	45BaO–5ZnO–40SiO <sub>2</sub> –10B <sub>2</sub> O <sub>3</sub>	–
Z2	40BaO–10ZnO–40SiO <sub>2</sub> –10B <sub>2</sub> O <sub>3</sub>	–
Z3	40BaO–15ZnO–35SiO <sub>2</sub> –10B <sub>2</sub> O <sub>3</sub>	–
Z4	40BaO–20ZnO–30SiO <sub>2</sub> –10B <sub>2</sub> O <sub>3</sub>	–
Z5	40BaO–25ZnO–25SiO <sub>2</sub> –10B <sub>2</sub> O <sub>3</sub>	–
Z6	20BaO–35ZnO–30SiO <sub>2</sub> –15B <sub>2</sub> O <sub>3</sub>	–
Z7	40BaO–10ZnO–35SiO <sub>2</sub> –15B <sub>2</sub> O <sub>3</sub>	50
Z8	40BaO–15ZnO–30SiO <sub>2</sub> –15B <sub>2</sub> O <sub>3</sub>	50
Z9	40BaO–20ZnO–25SiO <sub>2</sub> –15B <sub>2</sub> O <sub>3</sub>	50
Z10	45BaO–30ZnO–10SiO <sub>2</sub> –15B <sub>2</sub> O <sub>3</sub>	30
Z11	45BaO–30ZnO–10SiO <sub>2</sub> –15B <sub>2</sub> O <sub>3</sub>	45
Z12	45BaO–40ZnO–0SiO <sub>2</sub> –15B <sub>2</sub> O <sub>3</sub>	30
Z13	45BaO–40ZnO–0SiO <sub>2</sub> –15B <sub>2</sub> O <sub>3</sub>	45
Z14	20BaO–35ZnO–30SiO <sub>2</sub> –15B <sub>2</sub> O <sub>3</sub>	20
Z15	10BaO–40ZnO–30SiO <sub>2</sub> –20B <sub>2</sub> O <sub>3</sub>	20
Z16	0BaO–50ZnO–30SiO <sub>2</sub> –20B <sub>2</sub> O <sub>3</sub>	20
Z17	45BaO–5ZnO–40SiO <sub>2</sub> –10B <sub>2</sub> O <sub>3</sub>	30

### 3. Results and discussion

#### 3.1. XRD and SEM analyses

The physical properties, e.g. dielectric and thermal properties, of LTCC materials are determined by the physical characteristics of major mineral phases. Due to the close correlation between the physical properties and the phase composition, the phase formation mechanism of the eutectic system BaO–ZnO–SiO<sub>2</sub>–B<sub>2</sub>O<sub>3</sub> needs to be examined. Fig. 1 represents the XRD patterns of the specimens Z1, Z4, Z17 and the slurry of the specimen Z1, respectively. As seen in Fig. 1, the slurry mainly contains a barium borate hydrate phase, a small quantity of a zinc borate phase and a residual barium hydroxide. Major mineral phases of the specimens Z1, Z4, Z17 are barium silicate and SiO<sub>2</sub> crystal phases whereas a barium borate phase and other borate compounds are not detected. It is estimated that the barium borate hydrate phase have completely transformed into a melting phase during sintering. Fig. 2 gives the DSC curves of two barium borate hydrates. It appears that the thermal evolution of the two barium borate hydrates basically covers three stages, i.e., dehydration, a series of chemical combinations and melting at the temperature below 900 °C. The results indicate

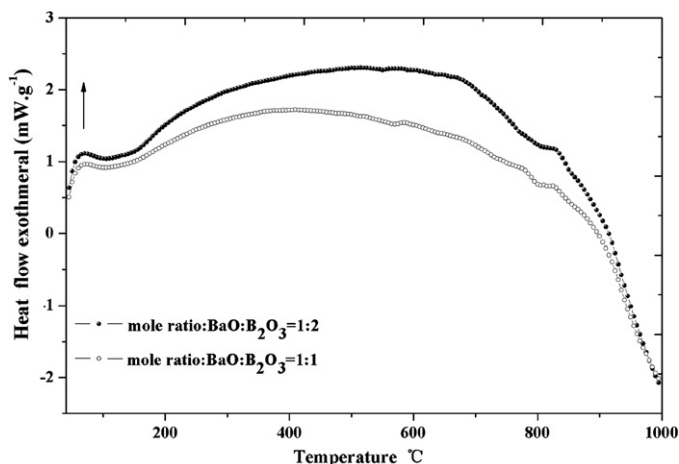


Fig. 2. DSC curves of two barium borate hydrates.

that a barium borate hydrate is characterized by low-melting characteristics. Due to the characteristics, barium borate can be usually used as a flux agent to improve the sintering behavior of ceramic materials [11]. Consequently, the phase formation in the eutectic system BaO–ZnO–SiO<sub>2</sub>–B<sub>2</sub>O<sub>3</sub> can be understood as the mechanism that, by a melting phase, various ions and polymer molecules are ineluctably dispersed and chemically combined with each other to form new polymorphs, the formation of the new bonds for the polymorphs also involves the structural rearrangement of the crystal particles to achieve a thermodynamic stability. Of these minerals, the occurrence of a SiO<sub>2</sub> crystal phase should be attributed to the crystallization of residual SiO<sub>2</sub> polymer molecules. It means that the phase formation depends on the chemical constitute.

For the investigation of the phase evolution dependence of the chemical constitute, the additional quartz and the oxide components in the eutectic system are examined in terms of their content in the specimen. As the specimens with high BaO and B<sub>2</sub>O<sub>3</sub> content and high quartz content, Fig. 3 gives the XRD patterns of the specimens Z7, Z8 and Z9, respectively. The XRD patterns show that their major phases are only quartz and a small quantity of SiO<sub>2</sub> crystal phases. The results indicate that the high content of BaO and B<sub>2</sub>O<sub>3</sub> in the composition can increase the amounts of the melting phase

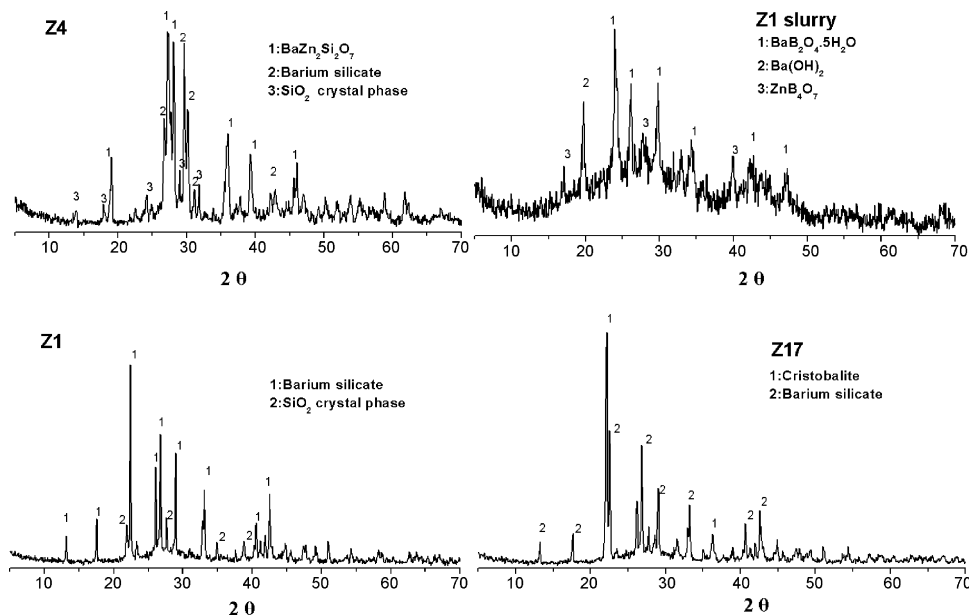


Fig. 1. XRD patterns of the specimens Z1, Z4, Z17 and the slurry of the specimen Z1.

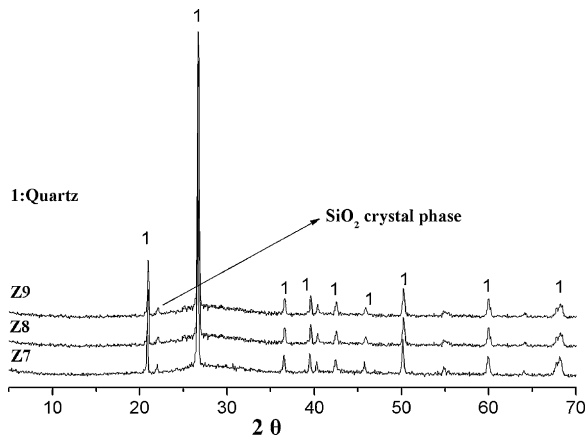


Fig. 3. XRD patterns of the specimens Z7, Z8 and Z9.

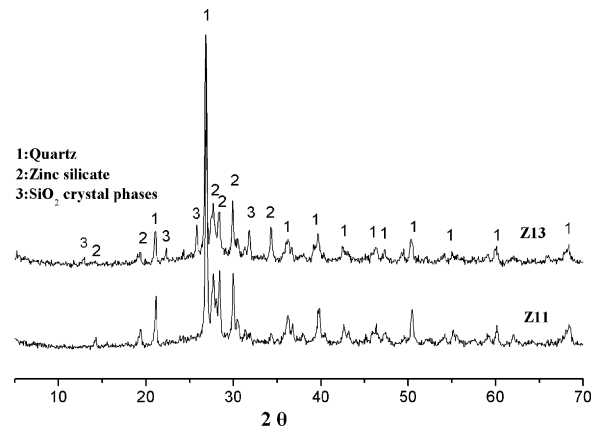


Fig. 5. XRD patterns of the specimens Z11 and Z13.

of barium borate in the composites. In turn, the other chemical constituents in the eutectic system can also transform accordingly into an amorphous phase via the dissolution of them to the melting phase. Usually, the presence of a melting phase in ceramic composites is beneficial to achieve a low-temperature sintering. Fig. 4 shows the correlation between the densification temperature and the composition. As is seen in Fig. 4, the specimens with high BaO and B<sub>2</sub>O<sub>3</sub> content (such as the specimens Z1–Z5) have a low densification temperature. It can be believed that the achievement of the low-temperature sintering mainly originated in the presence of the melting phase of a barium borate in the eutectic system. Consequently, the matrixes containing sufficient amounts of the melting phases have better ability to host quartz particles. In contrast to BaO and B<sub>2</sub>O<sub>3</sub>, adding quartz to the matrix can urge a higher densification temperature (such as the specimens Z7, Z8, Z9, Z11, Z13 and Z17). Therefore, in order to achieve a low-temperature sintering, the content of quartz in the composite materials needs to be reasonably regulated.

While the SiO<sub>2</sub> content in the matrixes of the specimens Z11 and Z13 is up to 10 wt.% and 0 wt.%, respectively. As seen in Fig. 5, major mineral phases of the specimens Z11 are quartz and zinc silicate. Generally, the formation of the zinc silicate phase is due to the chemical combination of Zn ion and SiO<sub>2</sub> polymer molecule in the eutectic system. However, a high ZnO content in the composition

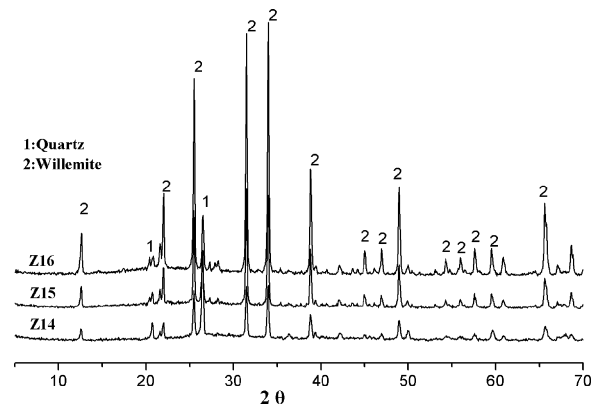


Fig. 6. XRD patterns of the specimens Z14, Z15 and Z16.

may result in the dissolution of the additional quartz to a melting phase and the formation of new silicate phases. In the XRD pattern of the specimen Z13, a zinc silicate phase and SiO<sub>2</sub> crystal phases can be observed. With the results, it indicates the fact that is the dissolution of quartz to a melting phase and the participation in the solid state reactions for the phase formation.

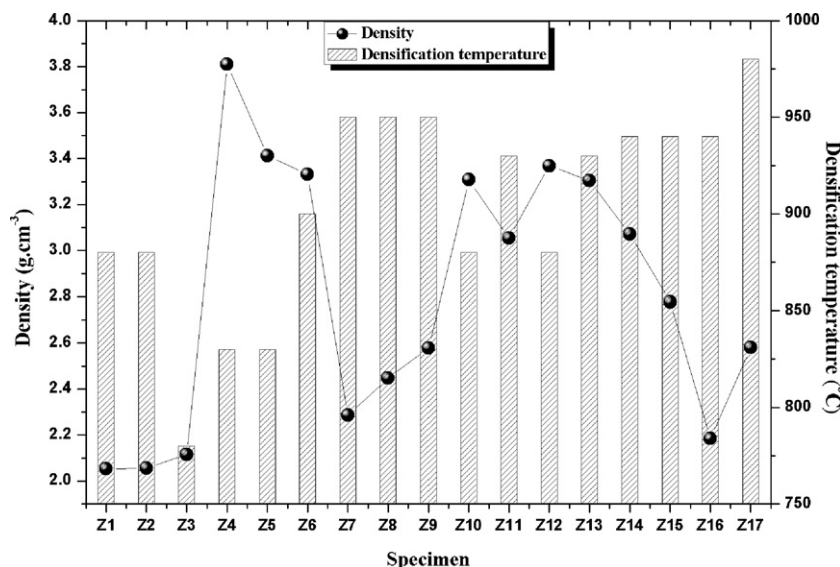


Fig. 4. Density and densification temperature of the matrix and composite specimens.

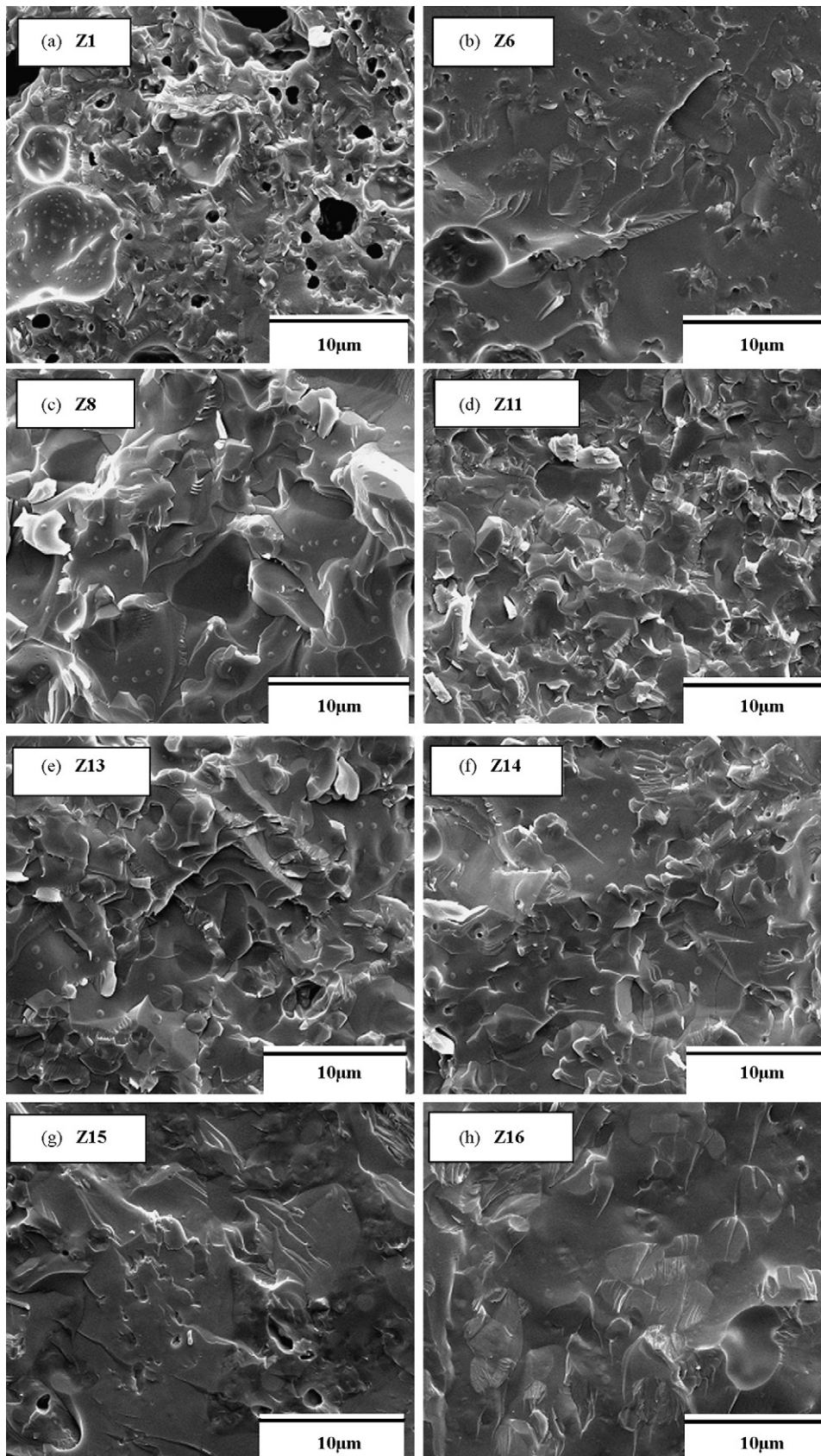


Fig. 7. SEM images of the matrix and composite specimens.

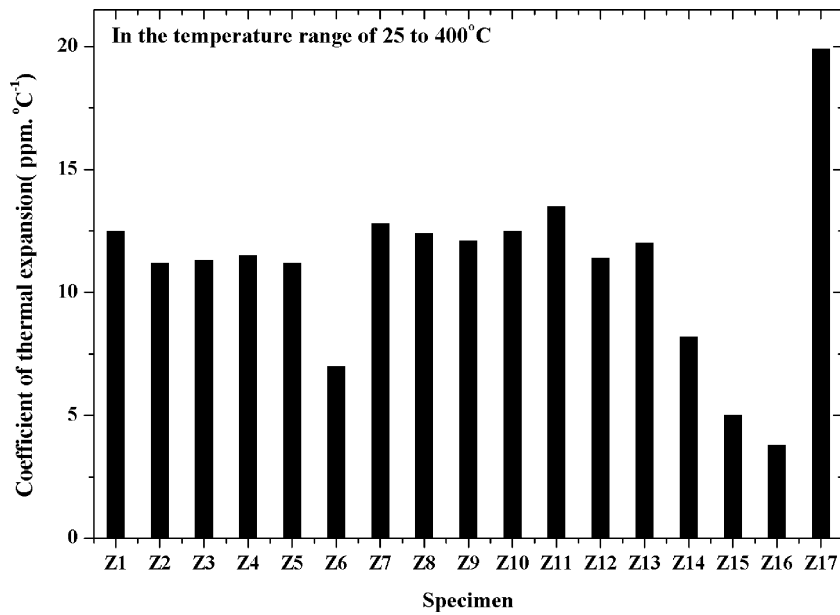


Fig. 8. Coefficient of thermal expansion of the matrix and composite specimens.

As the phase evolution dependence of the ZnO content in the matrix, Fig. 6 gives the XRD patterns of the specimens Z14, Z15 and Z16 with ZnO fraction in the amounts of 35 wt.%, 40 wt.% and 50 wt.%, respectively. The results indicate that major mineral phases of the three specimens are willemite and quartz. The intensity of the diffraction spectra of willemite is getting stronger with the increase of ZnO fraction in the matrix. Under this variation, the intensity of the diffraction spectra of quartz become gradually weak, indicating that the dissolution of quartz to the melting phase is occurring during sintering. Bunting and Sang [12,13] reported the formation of a willemite phase is attributed to the chemical combination of zinc silicate and SiO<sub>2</sub> crystal particles. Thus, adding quartz to the matrix and increasing ZnO fraction can cause the formation of a willemite phase. Because of the fact that the content of the melting phases increases as the content of BaO and B<sub>2</sub>O<sub>3</sub> in the eutectic system increases, the addition of quartz has been greatly decreased with the decrease of the BaO content in the three specimens.

Fig. 7 shows the SEM images of several specimens. As shown in Fig. 7, the SEM images of the specimens Z8, Z11 and Z13 exhibit a compacted microstructure. It indicates that the barium borate hydrate phase plays an important role in the improvement of the sintering behavior of the composite. The micrographs of the specimens Z14, Z15 and Z16 appear that, with the increase of the ZnO content, a willemite phase is gradually formed from the eutectic system during sintering. In addition, the porosity is observed in the SEM image of the specimen Z1 that contains BaO and B<sub>2</sub>O<sub>3</sub> fraction in the amounts of 55 wt.%. It is estimated that, due to a low soften point of the melting phase, the porosity is caused by the thermal swell of the specimen with excessive melting phase during sintering. Naturally, it results in a low density. Meanwhile, some dots are observed in the SEM images of the specimens Z1, Z8, Z13 and Z14. In contrast with the XRD results of the specimens, the dots could be SiO<sub>2</sub> crystal particles that originated from the crystallization of residual SiO<sub>2</sub> polymer component. Furthermore, the occurrence of

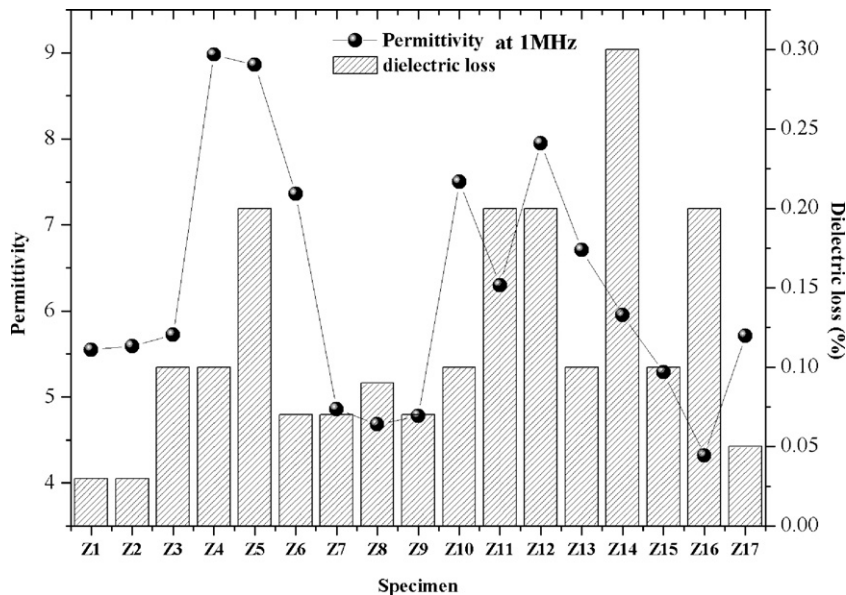


Fig. 9. Dielectric properties of the matrix and composite specimens.

the SiO<sub>2</sub> crystal particles in the specimen Z13, which does not contain the SiO<sub>2</sub> polymer component, is correlated with the dissolution of quartz to a melting phase. However, the micrograph of the specimen Z11 with the SiO<sub>2</sub> polymer component in amounts 10 wt.% does not show the dots. It suggests that the origination of the SiO<sub>2</sub> crystal phase is complicated and should be relevant with the proportion of the oxides in the composition [14]. In the case of the origination of the SiO<sub>2</sub> crystal phase, the further work will be done in future.

### 3.2. Dielectric and thermal properties of the composite

CTE values and dielectric properties of the specimens are represented in Figs. 8 and 9, respectively. As is shown in Figs. 8 and 9, the specimens with a high SiO<sub>2</sub> and BaO content possess high CTE value whereas the specimens with a high SiO<sub>2</sub> content express excellent dielectric properties. However, the influence of the ZnO component on the CTE and the dielectric properties is not clearly shown on the correlation between the composition and the properties. It means that the physical properties are relevant with the phase composition. Major mineral phases of the eutectic system BaO–ZnO–SiO<sub>2</sub>–B<sub>2</sub>O<sub>3</sub> are barium silicates, willemite and SiO<sub>2</sub> crystal phases. Of these mineral phases, barium silicates possess high CTE value (up to 12.5 ppm °C<sup>-1</sup>, in the temperature range of 20–300 °C) [15]. Thus, it is widely applied to glass–ceramic materials with high CTE (patent No. 3,467,534 U.S.A.). It can be seen that the specimens (such as Z1 and Z4) containing a barium silicate phase show a considerable CTE value. It is well known [10,16] that cristobalite is characterized by prominent CTE (up to 50 ppm °C<sup>-1</sup>, in the temperature range of 20–300 °C). Due to the presence of a cristobalite phase, the specimen Z17 has higher CTE value than the other specimens. As one of the major mineral phases, willemite possesses low CTE and permittivity ( $\epsilon_r = 6.6$ ,  $\tau_f = -61$  ppm °C<sup>-1</sup>) [17–20]. Therefore, the permittivity and the CTE value of the specimens Z14, Z15 and Z16 are decreasing with increasing the amounts of the willemite phase in the composites. On the other hand, the specimens (Z7, Z8 and Z9) with high quartz content express high CTE value and excellent dielectric properties. In consequence, it can be concluded that thermal and dielectric properties of the composite are decided mainly by the phase composition.

In general, because of the eutectic system with the wide eutectic areas and the multitude mineral phase areas, not only the

design of the physical properties but also the process is very convenient.

## 4. Conclusions

The present work has investigated the phase formation and the physical properties of the LTCC composite based on the eutectic system BaO–ZnO–SiO<sub>2</sub>–B<sub>2</sub>O<sub>3</sub>. It indicates that dielectric and thermal properties depend mainly on their major mineral phases. The presence of a barium silicates phase in the eutectic system is advantage to achieve a considerable CTE whereas the formation of a willemite phase can availably lower the permittivity of the composite. The difference is that the addition of quartz to the eutectic system and the emergence of SiO<sub>2</sub> crystal phases in the composite is not only helpful to increase CTE, but also is advantage to obtain excellent dielectric properties. According to the particular physical characteristics of these major mineral phases, the dielectric and thermal properties of the LTCC composite can be availably regulated.

## References

- [1] Y. Imanaka, Multilayered Low Temperature Co-fired Ceramic (LTCC) Technology, Springer, New York, 2005.
- [2] C. Bienert, A. Roosen, J. Eur. Ceram. Soc. 30 (2010) 369–374.
- [3] M. Eberstein, C. Glitzky, M. Gemeinert, T. Rabe, W.A. Schiller, Int. J. Appl. Ceram. Technol. 6 (2009) 1–8.
- [4] R. Wang, J. Zhou, B. Li, L. Li, J. Alloys Compd. 490 (2010) 204–207.
- [5] G.-H. Chen, L.-J. Tang, J. Cheng, M.-H. Jiang, J. Alloys Compd. 478 (2009) 858–862.
- [6] M.A. Vartanyan, E.S. Lukin, N.A. Popova, Glass Ceram. 56 (2008) 1–2.
- [7] C.-L. Huang, C.-L. Pan, W.-C. Lee, J. Alloys Compd. 462 (2008) L5–L8.
- [8] S.-F. Wang, Y.-R. Wang, Y.-C. Wu, Y.-J. Liu, J. Alloys Compd. 480 (2009) 499–504.
- [9] X. Chen, D. Chen, P. Lv, F. Yan, Z. Zhan, B. Li, F. Huang, J. Liang, J. Alloys Compd. 476 (2009) 241–244.
- [10] P.W. McMillan, Glass–ceramics, Academic Press, London, New York, 1964.
- [11] K. Singh, A. Inadurkar, Bull. Mater. Sci. 11 (1988) 55–61.
- [12] E.N. Bunting, J. Am. Ceram. Soc. 13 (1930) 5–10.
- [13] S.O. Yoon, T.H. Jo, K.S. Kim, S. Kim, Ceram. Int. 34 (2008) 2155–2157.
- [14] M.J. Jackson, B. Mills, J. Mater. Sci. 32 (1997) 5295–5304.
- [15] I.W. Donald, J. Mater. Sci. 28 (1993) 2841–2886.
- [16] S.J. Stevens, R.J. Hand, J.H. Sharp, J. Therm. Anal. 49 (1997) 1409–1415.
- [17] Y. Guo, H. Ohsato, K. Kakimoto, J. Eur. Ceram. Soc. 26 (2006) 1827–1830.
- [18] D.-N. Kim, J.-Y. Lee, J.-S. Huh, H.-S. Kim, J. Non-Cryst. Solids 3006 (2002) 70–75.
- [19] G.-H. Chen, X.-Y. Liu, J. Alloys Compd. 431 (2007) 282–286.
- [20] S.-G. Kim, J.-S. Park, K.S. Hong, H.-S. Kim, J. Electroceram. 15 (2005) 129–134.